Probabilistic properties of detrended fluctuation analysis for Gaussian processes

Grzegorz Sikora [*]
Faculty of Pure and Applied Mathematics, Hugo Steinhaus Center, Wroclaw University of Science and Technology, 50-370 Wroclaw, Poland

Marc Höll [†]
Department of Physics, Institute of Nanotechnology and Advanced Materials, Bar-Ilan University, Ramat-Gan, 5290002 Israel

Janusz Gajda [‡]
Faculty of Economic Sciences, University of Warsaw, 00-241 Warsaw, Poland

Holger Kantz [§]
Max Planck Institute for the Physics of Complex Systems, 01187 Dresden, Germany

Aleksei Chechkin [‖]
Institute of Physics & Astronomy, University of Potsdam, D-14476 Potsdam-Golm, Germany
and Akhiezer Institute for Theoretical Physics NSC "Kharkov Institute of Physics and Technology", 61108 Kharkov, Ukraine

Agnieszka Wyłomańska [¶]
Faculty of Pure and Applied Mathematics, Hugo Steinhaus Center, Wroclaw University of Science and Technology, 50-370 Wroclaw, Poland

(Received 11 September 2019; accepted 11 February 2020; published 11 March 2020)

Detrended fluctuation analysis (DFA) is one of the most widely used tools for the detection of long-range dependence in time series. Although DFA has found many interesting applications and has been shown to be one of the best performing detrending methods, its probabilistic foundations are still unclear. In this paper, we study probabilistic properties of DFA for Gaussian processes. Our main attention is paid to the distribution of the squared error sum of the detrended process. We use a probabilistic approach to derive general formulas for the expected value and the variance of the squared fluctuation function of DFA for Gaussian processes. We also get analytical results for the expected value of the squared fluctuation function for particular examples of Gaussian processes, such as Gaussian white noise, fractional Gaussian noise, ordinary Brownian motion, and fractional Brownian motion. Our analytical formulas are supported by numerical simulations. The results obtained can serve as a starting point for analyzing the statistical properties of DFA-based estimators for the fluctuation function and long-memory parameter.

DOI: 10.1103/PhysRevE.101.032114

I. INTRODUCTION

Detrended fluctuation analysis (DFA) was introduced in 1994 by Peng *et al.* for analyzing DNA sequences [1]. The DFA method is very popular in various fields of science and engineering since it is one of the most widely used techniques for detection of long-range dependence (called also long memory) in time series [2–8]. Such dependence is defined via the autocorrelation function $C(s)$ with a time lag s of a time series. If the summation over all time lags diverges then the time series is called long-range dependent. This property reflects the asymptotic power-law decay of the autocorrelation function, $C(s) \sim s^{-\delta}$, with the long-memory parameter $\delta \in (0, 1]$ [9,10].

If the summation converges the process is called short-range dependent. In order to estimate δ of a time series, one can use the estimator of the autocorrelation function. Unfortunately, this approach has several practical drawbacks, especially for a small number of data points [11,12]. A possible solution is to introduce another time-averaged statistic which may characterize the memory properties. One of the most powerful statistics is the fluctuation function $F(s)$ of the DFA. It provides an indirect way of estimating the long-memory parameter δ. The time axis is divided into segments of length s. In every segment v the squared error sum $f^2(v, s)$ between the summed time series and the polynomial fit is calculated. The squared fluctuation function is the average of these squared error sums and scales as $F^2(s) \propto s^{2\alpha}$ with fluctuation parameter α, which is connected to δ via $\alpha = 1 - \delta/2$ and to an anomalous diffusion exponent, as in, e.g., fractional Brownian motion (FBM). For large s the power-law behavior of the squared fluctuation function of the DFA can be seen more

*grzegorz.sikora@pwr.edu.pl
†hoell@pks.mpg.de
‡jgajda@wne.uw.edu.pl
§kantz@pks.mpg.de
‖chechkin@uni-potsdam.de
¶agnieszka.wylomanska@pwr.edu.pl

easily in a log-log plot than the power law of $C(s)$, because $F^2(s)$ is an increasing function with respect to s. Another important property of the DFA is its ability to remove the influence of external trends on the estimation of α whereas the sample autocorrelation function estimates δ only for stationary time series. All these abilities of DFA in addition with its easy implementation made it a successful tool for data analysis over the years.

Despite its success, there are only a few articles investigating the probabilistic properties of DFA. In fact, the main focus of most analytical studies of DFA is the scaling behavior [12–17] and the relationship to known statistical quantities [11,18–26]; see [26] for a detailed description of these articles. The asymptotic scaling behavior of the squared fluctuation function and the linear regression estimator for the parameter α have been studied in [27] for fractional Gaussian noise. Furthermore, in [26] it was derived that the squared error sums $f^2(v,s)$ are identical to weighted squared displacements of the summed time series. The procedure of detrending is then attributed to these weights, which allows one to explain detrending not only for external polynomial trends but also for fractional Brownian motion. However, the probabilistic properties of the squared error sum and fluctuation function have not been explored in detail.

In this paper, we study probabilistic properties of the squared fluctuation function of DFA for a general family of Gaussian processes. In fact, the fluctuation function of DFA, calculated on a finite data set, is a random variable itself with a yet unknown distribution. Using the theory of quadratic forms of Gaussian processes we find the distribution of the squared error sum of the detrended process. In contrast to the papers mentioned above, where only the asymptotic behavior of the expected value and the variance of the squared fluctuation function are considered, we proved the exact formulas for those quantities for general centered Gaussian process.

This paper continues the authors' recent research on another time-averaged statistic, namely time-averaged mean squared displacement, for the Gaussian processes [28] and serves as a starting point for the analysis of the statistical properties of the DFA-based estimators for fluctuation parameter α and the long-memory parameter δ. In this article, we present general formulas for the expected value and the variance of the squared fluctuation function for arbitrary order q of detrending. For the exemplary Gaussian processes we demonstrate the results for the cases $q=0$ and $q=1$.

II. EXPECTED VALUE AND VARIANCE OF SQUARED FLUCTUATION FUNCTION FOR GAUSSIAN PROCESSES

In what follows we consider the centered Gaussian process $\{Z(t)\}$ and the corresponding time series $\{Z(1), Z(2), \dots, Z(N)\}$. We define a path time series as a cumulative sum of the time series $\{Z(1), Z(2), \dots, Z(N)\}$:

$$X(t)=\sum_{i=1}^{t} Z(i), \quad t=1,2,\dots,N. \tag{1}$$

The time series $\{X(1), X(2), \dots, X(N)\}$ is also a centered Gaussian. We denote its covariance matrix as $\Sigma=\{E[X(i)X(j)]: i,j=1,2,\dots,N\}$. The procedure of detrended fluctuation analysis is based on the time series $\{X(1), X(2), \dots, X(N)\}$ and consists of several steps. First, the time axis $1,2,\dots,N$ is divided into K segments of length s, $K=[N/s]$. In every segment v, $v=1,2,\dots,K$, we derive the squared error sum of the detrended process $f^2(v,s)$ as

$$\begin{aligned} f^2(v,s) &= \frac{1}{s}\sum_{t=1+d_v}^{s+d_v}[X(t)-p_v(t)]^2 \\ &= \frac{1}{s}\sum_{t=1}^{s}[Y_v(t)]^2=\mathbb{Y}_v\mathbb{Y}_v^T, \end{aligned} \tag{2}$$

where $p_v(\cdot)$ is the fitting polynomial of order q in the segment v obtained by ordinary least-squares method and $d_v=(v-1)s$. The vector $\mathbb{Y}_v=\{Y_v(t): t=1,\dots,s\}$ has the components $Y_v(t)=X(t+d_v)-p_v(t+d_v)$. The order q of $p_v(\cdot)$ is a free parameter. The first three orders of constant, linear, and quadratic detrending, $q=0$, 1, and 2, are the ones which are mostly used in practical applications. Finally, the square of the fluctuation function of DFA is the average over all the squared error sums:

$$F^2(s)=\frac{1}{K}\sum_{v=1}^{K} f^2(v,s)=\frac{1}{[N/s]}\sum_{v=1}^{[N/s]} f^2(v,s). \tag{3}$$

In this paper, we provide the formulas for arbitrary q and get explicit results for $q=0$ and 1. The fit of order q is $p_v(t)=\sum_{m=0}^{q}\hat{a}_{m,v}t^m$. The coefficients $\hat{a}_{m,v}$ can be calculated directly from the system of linear equations

$$\begin{pmatrix}\hat{a}_{0,v}\\ \vdots\\ \hat{a}_{q,v}\end{pmatrix}=\begin{pmatrix}S_{0,v} & \cdots & S_{q,v}\\ \vdots & \ddots & \vdots\\ S_{q,v} & \cdots & S_{2q,v}\end{pmatrix}^{-1}\begin{pmatrix}\sum_{i=1+d_v}^{s+d_v}X(i)\\ \vdots\\ \sum_{i=1+d_v}^{s+d_v} i^q X(i)\end{pmatrix} \tag{4}$$

with $S_{j,v}=\sum_{i=1+d_v}^{s+d_v} i^j$, $j=0,1,2$. Using Eq. (4) the fit can be written as a weighted sum of $X(i)$, $i=1+d_v,\dots,s+d_v$:

$$p_v(t)=\sum_{i=1+d_v}^{s+d_v} X(i)P_v(i,t). \tag{5}$$

The weights are defined as

$$P_v(i,t)=\sum_{m,n=0}^{q} t^m i^n\left(\mathbb{S}_v^{-1}\right)_{m+1,n+1}, \tag{6}$$

where $\mathbb{S}_v^{-1}$ is the inverse matrix of the matrix $\mathbb{S}_v$ with the elements $(\mathbb{S}_v)_{m,n}=S_{m+n-2,v}$. From Eqs. (5) and (6) we get

$$Y_v(t)=\sum_{i=1}^{s} X(i+d_v)[\delta_{i,t}-P_v(i+d_v,t+d_v)], \tag{7}$$

with $\delta_{\cdot,\cdot}$ being the Kronecker delta and $i,t=1,2,\dots,s$. The weights $P_v(i+d_v,t+d_v)$ can be expressed in explicit form for zeroth order of detrending $q=0$ as

$$P_v(i+d_v,t+d_v)=\frac{1}{s} \tag{8}$$

and for first order of detrending $q=1$ as

$$\begin{aligned} &P_v(i+d_v,t+d_v)\\ &\quad=\frac{6i(2t-s-1)+2(s+1)(-3t+2s+1)}{s^3-s}. \end{aligned} \tag{9}$$

It is also possible to calculate the weights for any higher order of detrending. It can be shown that $P_v(i+d_v, t+d_v)$ does not depend on the number v of the segment. Thus Eq. (7) can be written as

$$Y_v(t) = \sum_{i=1}^{s} X(i+d_v)[\delta_{i,t} - P_1(i,t)]. \quad (10)$$

The covariance $E[Y_v(m)Y_u(n)]$, $m, n = 1, 2, \ldots, s$ of the vectors $\mathbb{Y}_v = \{Y_v(t) : t = 1, \ldots, s\}$ and $\mathbb{Y}_u = \{Y_u(t) : t = 1, \ldots, s\}$ for each $v, u = 1, 2, \ldots, [N/s]$ has the form

$$E[Y_v(m)Y_u(n)] = \sum_{i,j=1}^{s} E[X(i+d_v)X(j+d_u)] \times [\delta_{i,m} - P_1(i,m)][\delta_{j,n} - P_1(j,n)]. \quad (11)$$

Let us go back to Eq. (2). According to the Gaussian quadratic forms theory [29], $sf^2(v,s)$ has a so-called generalized χ^2-squared distribution, namely

$$sf^2(v,s) \overset{d}{=} \sum_{j=1}^{s} \lambda_j(v)U_j, \quad (12)$$

where U_j's are independent identically distributed random variables having χ^2 distribution with one degree of freedom, $E[U_j] = 1$, $\mathrm{Var}\,[U_j] = 2$, and weights $\lambda_j(v)$ are the eigenvalues of the covariance matrix $\Sigma_{\mathbb{Y}_v} = \{E[Y_v(m)Y_v(n)] : m, n = 1, \ldots, s\}$; see Eq. (11). Therefore, for random quantity $f^2(v,s)$ the expected value and the variance are as follows:

$$E[f^2(v,s)] = \frac{1}{s}\sum_{j=1}^{s} \lambda_j(v) = \frac{1}{s}\mathrm{tr}(\Sigma_{\mathbb{Y}_v}) = \frac{1}{s}\sum_{j=1}^{s} E[Y_v^2(j)], \quad (13)$$

$$\mathrm{Var}[f^2(v,s)] = \frac{2}{s^2}\sum_{j=1}^{s} \lambda_j^2(v) = \frac{2}{s^2}\mathrm{tr}\left(\Sigma_{\mathbb{Y}_v}^2\right) = \frac{2}{s^2}\sum_{i,j=1}^{s} \{E[Y_v(i)Y_v(j)]\}^2. \quad (14)$$

To get (13) and (14) we use two important facts from linear algebra, namely (i) the sum of all eigenvalues of a given matrix is equal to the trace of that matrix, and (ii) the sum of squared eigenvalues of a given matrix is the trace of this matrix taken to the power 2 [30]. Equations (13) and (14) are the first main result of the paper.

Notice that the distribution of the quadratic form $sf^2(v,s)$ given in (12) can be represented as a sum of s independent gamma distributed random variables with constant shape parameter $1/2$ and different scale parameters [31]. Namely

$$sf^2(v,s) \overset{d}{=} \sum_{j=1}^{s} G(1/2, 2\lambda_j(v)), \quad (15)$$

where $G(k,\theta)$ is the gamma distributed random variable with parameters k and θ. The characteristic function, the moment generating function, and the probability density function for $f^2(s,v)$ are presented in Appendix A 1.

The expected value and the variance of the squared error sum of the detrended process $f^2(v,s)$ allow calculating the same quantities for the squared fluctuation function $F^2(s)$. Namely, the expected value of the $F^2(s)$ takes the form

$$E[F^2(s)] = \frac{1}{[N/s]}\sum_{v=1}^{[N/s]} E[f^2(v,s)] = \frac{1}{s[N/s]}\sum_{v=1}^{[N/s]}\sum_{j=1}^{s} E\big[Y_v^2(j)\big], \quad (16)$$

where the last equality comes from formula (13) and $E[Y_v^2(j)]$ can be calculated with formula (11) with $v = u$. Respectively, the variance of $F^2(s)$ has the form

$$\mathrm{Var}[F^2(s)] = \frac{2}{s^2[N/s]^2}\sum_{v,u=1}^{[N/s]}\sum_{t,w=1}^{s}[E[Y_v(t)Y_u(w)]]^2, \quad (17)$$

where $E[Y_v(t)Y_u(w)]$ is calculated according to the formula (11). The details of the derivation are presented in Appendix A 2. Equations (16) and (17) are our second main result. We stress again that Eqs. (13) and (14) as well as (16) and (17) are valid for any value of parameter q.

III. EXPECTED VALUE OF SQUARED FLUCTUATION FUNCTION FOR EXEMPLARY GAUSSIAN PROCESSES

In this section, we present behavior of the expected value of the squared fluctuation function for selected Gaussian processes for detrending parameters $q = 0$ and $q = 1$. We also illustrate the theoretical results by numerical simulations.

A. Gaussian white noise

As the first example we consider the path time series $\{X_1(1), X_1(2), \ldots, X_1(N)\}$ of Gaussian white noise $WN(0, \sigma^2)$, that is the process $\{X_1(t)\}$ with $E[X_1(t)] = 0$ and the autocovariance function given by

$$E[X_1(t)X_1(t+\tau)] = \begin{cases} \sigma^2 & \text{if } \tau = 0, \\ 0 & \text{if } \tau \neq 0. \end{cases} \quad (18)$$

Using Eq. (16) for $WN(0,1)$ we obtain

$$E[F^2(s)] = \frac{s-1}{s} \quad (19)$$

for $q = 0$, while

$$E[F^2(s)] = \frac{s-2}{s} \quad (20)$$

for $q = 1$. The details are presented in Appendix A 3. Equation (20) is an exact result which, to the best of our knowledge, was not obtained before. This is our third main result.

In Fig. 1 we demonstrate a comparison between the theoretical expected value of the squared fluctuation function for $WN(0,1)$ given in (20) and the empirical one for $q = 1$ for the simulated trajectories of the considered process. As one can see, the theoretical and empirical expectations coincide.

B. Fractional Gaussian noise

As the second example we consider the path time series $\{X_2(1), X_2(2), \ldots, X_2(N)\}$ of fractional Gaussian noise

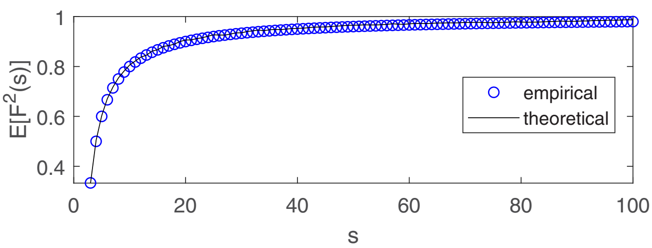

FIG. 1. The comparison between theoretical and empirical expected values of the squared fluctuation function for $q = 1$ for $WN(0, 1)$ for $N = 100$ (the time series length). The number of Monte Carlo simulations is $M = 500$.

(FGN). The FGN is a stationary process which defined heuristically as the derivative of the fractional Brownian motion [32–34]. The autocovariance function of FGN is given by

$$E[X_2(t)X_2(t+\tau)] = D\frac{(\tau+1)^{2H} - 2\tau^{2H} + |\tau-1|^{2H}}{2}, \tag{21}$$

where parameter $H \in (0, 1)$ is the Hurst exponent, and $D > 0$ is the diffusion coefficient. In our consideration we assume for simplicity $D = 1$. Notice that for $H = 0.5$ the FGN reduces to the white noise process considered above. Using Eq. (16) we obtain that for FGN with $D = 1$ and $H \neq 0.5$ the expectation of $F^2(s)$ for large s behaves as

$$E[F^2(s)] \approx 1 - s^{2H-2} \tag{22}$$

for $q = 0$, while

$$E[F^2(s)] \approx 1 - 2\frac{2-H}{H+1}s^{2H-2} \tag{23}$$

for $q = 1$. The details are presented in Appendix A 4. Equation (23) is the fourth main result of the paper.

In Fig. 2 we demonstrate the empirical means of the squared fluctuation function (circle lines) for FGN for $q = 1$ for two selected values of the H parameter: $H = 0.3$ (top panel) and $H = 0.7$ (bottom panel). Moreover, in Fig. 2 we present also the theoretical approximation given by the right-hand side of (23). As one can see, for both cases the empirical means of the squared fluctuation function and the theoretical means coincide.

C. Ordinary Brownian motion

As the third example we analyze the path time series $\{X_3(1), X_3(2), \ldots, X_3(N)\}$ which represents the trajectory of ordinary Brownian motion (OBM), that is a Gaussian process with stationary independent increments. The autocovariance function of OBM is given by

$$\mathbb{E}[X_3(t)X_3(t+\tau)] = 2Dt, \quad t, \tau > 0, \tag{24}$$

where $D > 0$. In further analysis we assume $D = 1/2$. Using formula (16) we obtain the exact value of the squared fluctuation function for OBM:

$$E[F^2(s)] = \frac{s^2-1}{6s} \tag{25}$$

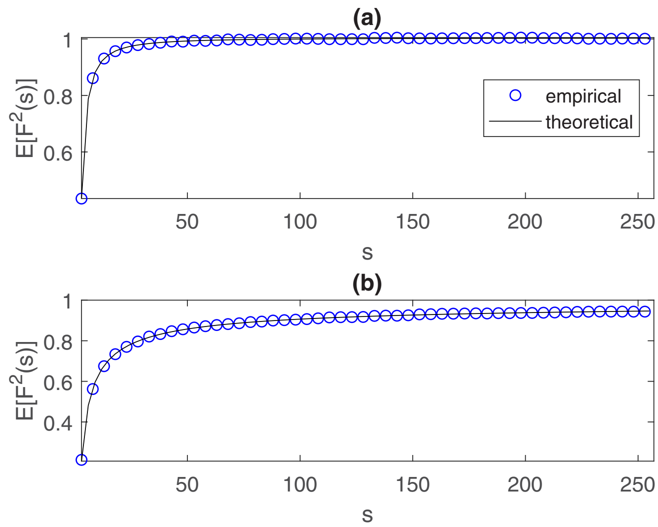

FIG. 2. The empirical mean of the squared fluctuation function $F^2(s)$ for $q = 1$ for FGN (circle lines) with $H = 0.3$ (top panel) and $H = 0.7$ (bottom panel) and the corresponding theoretical ones (solid line). The trajectory length $N = 256$ and the number of Monte Carlo simulations used to calculate the empirical mean is $M = 500$.

for $q = 0$, while

$$E[F^2(s)] = \frac{s^2-4}{15s} \tag{26}$$

for $q = 1$ with $s > 2$. The details are presented in Appendix A 5. Equations (25) and (26) reproduce the result that was obtained earlier by a different method in Ref. [11]. In the present paper we rederive it by using the general analytical technique developed in Sec. II.

In Fig. 3 we demonstrate a comparison between the empirical expected value for the squared fluctuation function for $q = 1$ for OBM and the theoretical one given by Eq. (26). As one can observe, the theoretical and empirical expectations coincide.

D. Fractional Brownian motion

As the last example, we consider the path time series $\{X_4(1), X_4(2), \ldots, X_4(N)\}$, which represents the trajectory of fractional Brownian motion [9,10]. The FBM is a centered Gaussian process with the self-similarity index (Hurst

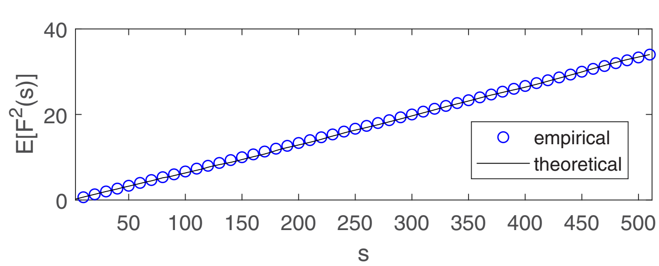

FIG. 3. The comparison between theoretical and empirical expected values of the squared fluctuation function for $q = 1$ for OBM for $D = 1$, $N = 512$. The number of Monte Carlo simulations is $M = 500$.

exponent) H, $0 < H < 1$. When $H < 1/2$ the increments of FBM are negatively correlated. For $H > 1/2$ the increments of FBM are positively correlated. The autocovariance function of FBM is given by

$$\mathbb{E}[X_4(t)X_4(t+\tau)] = D(t^{2H} + (t+\tau)^{2H} - |\tau|^{2H}), \tag{27}$$

where $D > 0$ is the diffusion coefficient. For simplicity, we assume $D = 1$. Using formula (16) for large s and $q = 0$ we obtain

$$E[F^2(s)] \approx \frac{2s^{2H}}{(2H+1)(2H+2)}, \tag{28}$$

while for $q = 1$ the following scaling holds:

$$E[F^2(s)] \propto s^{2H}, \quad s \to \infty. \tag{29}$$

The detailed calculations are presented in Appendix A 6. Equation (29) reproduces the asymptotic behavior that was derived earlier in [11,13,14,16,27]. It is worthwhile to note that similar to [13,27] our approach here allows us to take the interdependence of the segments, which are sections of a single time series, into account explicitly. This is important since for nonstationary processes it is not *a priori* clear that Eq. (3) is an average over identically distributed terms; see also [26]. If the signal is the additive composition of a fluctuating part $z_1(t)$ plus a systematic trend $z_2(t)$, $Z(t) = z_1(t) + z_2(t)$, then the fluctuation function (and hence also its expectation value) is the sum of the fluctuation functions of $z_1(t)$ and $z_2(t)$. The detrending procedure is intended to suppress the contribution of $z_2(t)$ in the signal and thereby to isolate the contribution of the fluctuating part of the signal. But even if there is no systematic trend on the time series, Eq. (2) requires subtracting a fitted polynomial from the sequence $X(t)$. So one might wonder whether this operation distorts the scaling exponent. It is necessary to consider the full segment dependent calculation as presented in Appendix A 6, which is a different approach than in [26] and hence another proof that detrending does not destroy the asymptotic scaling behaviour of FBM.

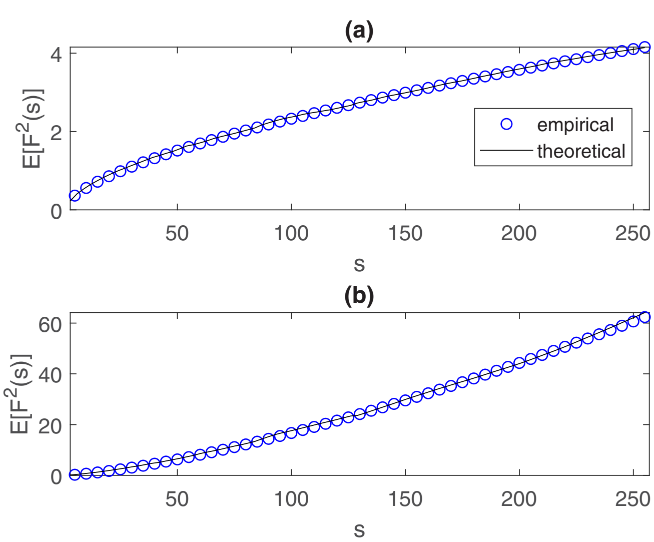

FIG. 4. The empirical means (circle line) of the squared fluctuation function for $q = 1$ for FBM for $H = 0.3$ (top panel) and $H = 0.7$ (bottom panel) and the corresponding theoretical expected values given by the right-hand side of Eq. (29) with fitted prefactor a of the functions as^{2H} by the least-squares method (the solid line). The trajectory length $N = 256$ and the number of Monte Carlo simulations used to calculate the empirical mean is $M = 500$.

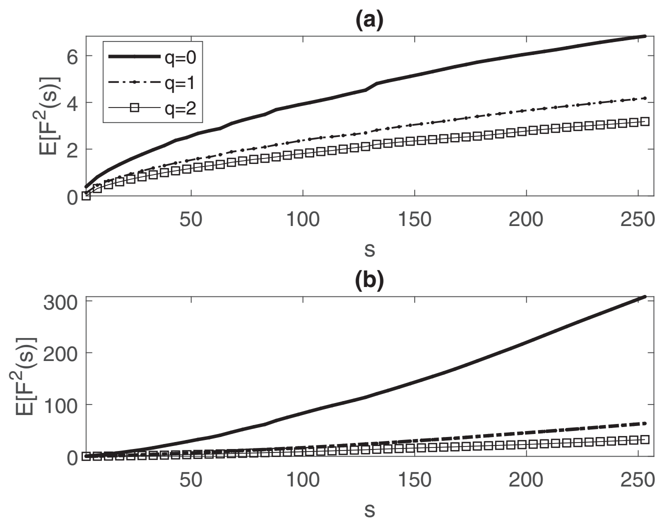

FIG. 5. The empirical means of the squared fluctuation function for $q = 0$, 1, and 2 for FBM with $H = 0.3$ (top panel) and $H = 0.7$ (bottom panel). The trajectory length $N = 256$ and the number of Monte Carlo simulations used to calculate the empirical mean is $M = 500$.

In Fig. 4 we demonstrate the empirical means (circle line) of the squared fluctuation function for $q = 1$ for FBM for two selected values of the H parameter, namely $H = 0.3$ (top panel) and $H = 0.7$ (bottom panel). We also present the corresponding theoretical expected values given by the right-hand side of Eq. (29) with fitted prefactor a of the functions as^{2H} by the least-squares method (the solid line) in order to demonstrate the asymptotic behavior of the considered quantity. One can see that the simulations confirm the theoretical result given in Eq. (29).

In order to demonstrate the influence of the order of detrending, namely the q parameter, on the expected value of the squared fluctuation function for FBM, in Fig. 5 we show the results for $q = 0$, 1, and 2. The corresponding expected values are calculated for the 500 simulated trajectories of FBM for $H = 0.3$ and $H = 0.7$. We see that the deviations of the asymptotic behavior of the expectation of the $F^2(s)$ statistic are much smaller between the cases $q = 1$ and $q = 2$ than between $q = 0$ and $q = 1$.

IV. CONCLUSIONS

The fluctuation function of DFA, evaluated with a single time series, is a random variable itself. In this paper we study its probabilistic properties. We present the distribution of the single time window squared error $f^2(\nu, s)$ for general centered Gaussian processes. From this expression we derive the variance of the fluctuation function $F^2(s)$, which can be used to define an s-dependent confidence intervals around the numerical results of DFA. We consider this as the first step towards the assessment of statistical estimation errors on the scaling exponent α of DFA. We have proved the formulas for the expected value and the variance of the squared fluctuation function for Gaussian processes and order of detrending. Based on that, we have analyzed the asymptotic behavior of the expectation of the $F^2(s)$ random variable for selected Gaussian processes for special cases of detrending. The theoretical results are confirmed by numerical simulation. The paper can be a starting point for studying probabilistic properties of the fluctuation parameter estimator.

The next key step in the theory will be to achieve analogous results for similar methods such as detrending moving average (DMA) [35–38] and for multifractal extensions, namely multifractal DFA (MF-DFA) [39] and multifractal DMA (MF-DMA) [40]. The method of DMA is well-established [5,7,41–48] and its detrending operation works similarly to DFA [26], which implies a natural application of our approach to DMA. Such extensions as MF-DFA [49,50] and MF-DMA [51,52] were recently applied to many diverse fields. To the best of our knowledge, the probabilistic properties of these methods have not been studied in detail yet. We hope that the methodology of this paper and the results presented will be useful for multifractal analysis as well.

ACKNOWLEDGMENTS

A.C. acknowledges financial support by the Deutsche Forschungsgemeinschaft (DFG Grant No. ME 1535/7-1). A.W. would like to acknowledge support by the National Center of Science Opus Grant No. 2016/21/B/ST1/00929 "Anomalous diffusion processes and their applications in real data modeling."

APPENDIX

1. Probability distribution of the squared error sum

The probability density function of gamma distributed random variable $G(k,\theta)$ with shape parameter k and scale parameter θ reads

$$h_{(k,\theta)}(x)=\frac{x^{k-1}\exp(-x/\theta)}{\Gamma(k)\,\theta^k},\quad x>0. \tag{A1}$$

The characteristic function of $G(k,\theta)$ is given by

$$\phi_{(k,\theta)}(t)=\frac{1}{[1-\theta it]^k}. \tag{A2}$$

Taking into account Eq. (15) one can see that the characteristic function of $sf^2(v,s)$ is a product of characteristic functions of gamma distributed random variables. Thus, the random variable $f^2(v,s)$ has the following characteristic function:

$$\phi_{v,s}(x)=E[\exp\{if^2(v,s)x\}]=\prod_{j=1}^{s}\frac{1}{[1-2\lambda_j(v)ix/s]^{1/2}}. \tag{A3}$$

The expressions for the moment generating function and the probability density function stem from the result of Ref. [31], which establishes such quantities for a linear combination of independent gamma random variables. In our case, such a linear combination is the statistic $sf^2(v,s)$; see Eq. (15). Thus the moment generating function for $f^2(s,v)$ takes the form

$$M_{v,s}(x)=E[\exp\{if^2(v,s)x\}]=C(1-2\lambda_1(v)x)^{-s/2}\exp\left(\sum_{k=1}^{\infty}\frac{\gamma_k}{(1-2\lambda_1(v)x)^k}\right), \tag{A4}$$

where $\lambda_1(v)$ is the smallest eigenvalue of the matrix $\Sigma_{\mathbb{Y}_v}$,

$$\gamma_k=\sum_{j=1}^{s}\frac{[1-\lambda_1(v)/\lambda_j(v)]^k}{2k}, \tag{A5}$$

and

$$C=\prod_{j=1}^{s}\left(\frac{\lambda_1(v)}{\lambda_j(v)}\right)^{1/2}. \tag{A6}$$

The probability density function for $f^2(s,v)$ is given by

$$g_{v,s}(x)=C\sum_{k=0}^{\infty}\frac{\Delta_k\,x^{\frac{s}{2}+k-1}\exp\left(-\frac{xs}{2\lambda_1(v)}\right)}{\Gamma\left(\frac{s}{2}+k\right)\left(\frac{2\lambda_1(v)}{s}\right)^{\frac{s}{2}+k}}, \tag{A7}$$

where Δ_k is expressed by the recursive formula

$$\Delta_{k+1}=\frac{1}{k+1}\sum_{j=1}^{k+1}j\gamma_j\Delta_{k+1-j},\quad \Delta_0=1. \tag{A8}$$

2. Variance of the squared fluctuation function

According to (3) the variance of $F^2(s)$ takes the form

$$\begin{aligned}\mathrm{Var}\left[F^2(s)\right]&=\frac{1}{[N/s]^2}\,\mathrm{Var}\left[\sum_{v=1}^{[N/s]}f^2(v,s)\right]\\&=\frac{1}{[N/s]^2}\sum_{v,u=1}^{[N/s]}\mathrm{Cov}[f^2(v,s),f^2(u,s)]\\&=\frac{1}{[N/s]^2}\sum_{v,u=1}^{[N/s]}E[f^2(v,s)f^2(u,s)]\\&\quad-\frac{1}{[N/s]^2}\sum_{v,u=1}^{[N/s]}E[f^2(v,s)]E[f^2(u,s)].\end{aligned} \tag{A9}$$

Using the fact that $\{X(1),X(2),\dots,X(N)\}$ is a time series of the general centered Gaussian process, we compute

$$\begin{aligned}E[f^2(v,s)f^2(u,s)]&=\frac{1}{s^2}E\left[\sum_{tw,=1}^{s}Y_v^2(t)Y_u^2(w)\right]\\&=\frac{1}{s^2}\sum_{t,=1}^{s}E\left[Y_v^2(t)Y_u^2(w)\right]\\&=\frac{1}{s^2}\sum_{t,w=1}^{s}E\left[Y_v^2(t)\right]E\left[Y_u^2(w)\right]\\&\quad+\frac{1}{s^2}\sum_{t,w=1}^{s}2\{E[Y_v(t)Y_u(w)]\}^2,\end{aligned} \tag{A10}$$

where the last equality follows from Isserlis's theorem for the fourth joint moment of the multivariate normal distribution [53]. By substituting (A10) and (13) into (A9) we get the variance given in (17).

3. Example: Gaussian white noise

Taking under consideration Eq. (16), the fact that the autocovariance function of white noise depends only on the time lag, and $E[X_1^2(t)] = 1$, we obtain

$$E[F^2(s)] = \frac{1}{s}\sum_{i,t=1}^{s}[\delta_{i,t} - P_1(i,t)]^2, \tag{A11}$$

where $P_1(\cdot,\cdot)$ is given in (9). Next, we will show that

$$\sum_{i,t=1}^{s}[\delta_{i,t} - P_1(i,t)]^2 = \sum_{i=1}^{s}\left(1 - 2P_1(i,i) + \sum_{t=1}^{s}P_1^2(i,t)\right). \tag{A12}$$

Indeed,

$$\begin{aligned}&\sum_{i,t=1}^{s}[\delta_{i,t} - P_1(i,t)]^2\\ &= \sum_{i=1}^{s}(1 - P_1(i,i))^2 + \frac{1}{s}\sum_{i=1}^{s}\sum_{t=1,t\neq i}^{s}P_1^2(i,t)\\ &= \sum_{i=1}^{s}\left(1 - 2P_1(i,i) + \sum_{t=1}^{s}P_1^2(i,t)\right).\end{aligned} \tag{A13}$$

Taking this formula along with the definition of the $P_1(\cdot,\cdot)$ function given in (8) for $q = 0$, we obtain

$$\sum_{i=1}^{s}\left(1 - 2P_1(i,i) + \sum_{t=1}^{s}P_1^2(i,t)\right) = s - 1. \tag{A14}$$

Taking Eq. (A13) along with the definition of $P_1(\cdot,\cdot)$ function given in (9) for $q = 1$ and using MATHEMATICA, we get

$$\sum_{i=1}^{s}\left(1 - 2P_1(i,i) + \sum_{t=1}^{s}P_1^2(i,t)\right) = s - 2. \tag{A15}$$

Thus, after plugging (A14) and (A15) into (A11) finally we obtain Eqs. (19) and (20).

4. Example: Fractional Gaussian noise

Taking under consideration Eq. (16) and the fact that the autocovariance function of FGN depends only on the time lag τ, we obtain

$$\begin{aligned}E[F^2(s)] &= \frac{1}{s}\sum_{i=1}^{s}E\left[X_2^2(i)\right]\left(1 - 2P_1(i,i) + \sum_{m=1}^{s}P_1^2(i,m)\right)\\ &+ \frac{2}{s}\sum_{\tau=1}^{s-1}E[X_2(1)X_2(1+\tau)]\sum_{i=1}^{s-\tau}\left(-2P_1(i,i+\tau)\right.\\ &\left.+\sum_{m=1}^{s}P_1(i,m)P_1(i+\tau,m)\right).\end{aligned} \tag{A16}$$

With $E[X_2^2(i)] = 1$ for $q = 0$ and $q = 1$ one can have

$$\begin{aligned}&\frac{1}{s}\sum_{i=1}^{s}E\left[X_2^2(i)\right]\left[1 - 2P_1(i,i) + \sum_{m=1}^{s}P_1^2(i,m)\right]\\ &= 1 - \frac{2}{s} \approx 1.\end{aligned}$$

In order to find the limit of the second component of the right-hand side of Eq. (A16), we use the fact that for $H \neq 0.5$

$$E[X_2(t)X_2(t+\tau)] \approx H(2H-1)\tau^{2H-2}. \tag{A17}$$

Applying formula (8) we obtain for $q = 0$

$$\begin{aligned}&\sum_{i=1}^{s-\tau}\left[-2P_1(i,i+\tau) + \sum_{m=1}^{s}P_1(i,m)P_1(i+\tau,m)\right]\\ &= -\frac{s-\tau}{s}.\end{aligned}$$

Thus, the second component of the right-hand side of Eq. (A16) for $q = 0$ takes the form

$$\begin{aligned}&-\frac{2}{s^2}H(2H-1)\sum_{\tau=1}^{s-1}\tau^{2H-2}(s-\tau)\\ &\approx -\frac{2s^{2H-1}}{s(2H-1)}H(2H-1) + \frac{2s^{2H}}{s^2 2H}H(2H-1)\\ &= s^{2H-2}(2H-1-2H) = -s^{2H-2}.\end{aligned} \tag{A18}$$

Thus finally we obtain Eq. (22).

In the case $q = 1$ with $E[X_2^2(i)] = 1$, applying (A17) and the definition of the $P_1(\cdot,\cdot)$ function given in (9) and using MATHEMATICA, we obtain

$$\begin{aligned}&\sum_{i=1}^{s-\tau}\left[-2P_1(i,i+\tau) + \sum_{m=1}^{s}P_1(i,m)P_1(i+\tau,m)\right]\\ &= -2 - 2\frac{\tau - 2s^2\tau + \tau^3}{s^3 - s}.\end{aligned} \tag{A19}$$

Thus, the second component of the right-hand side of Eq. (A16) for $q = 1$ takes the form

$$\frac{4}{s}H(2H-1)\sum_{\tau=1}^{s-1}\tau^{2H-2}\left(-1 - \frac{1-2s^2}{s^3-s}\tau - \frac{\tau^3}{s^3-s}\right). \tag{A20}$$

In order to calculate the above sum, we use the known approximation [14]

$$\sum_{t=1}^{m}t^h \approx \frac{m^{h+1}}{h+1} \quad \text{for large } m \text{ and } h \neq -1. \tag{A21}$$

Moreover, for large s we have

$$\frac{2s^2-1}{s^3-s} \approx 2/s \quad \text{and} \quad \frac{1}{s^3-s} \approx 1/s^3. \tag{A22}$$

Thus, for large s, Eq. (A20) takes the form

$$\frac{4}{s}H(2H-1)\sum_{\tau=1}^{s-1}\tau^{2H-2}\left(-1-\frac{1-2s^2}{s^3-s}\tau-\frac{1}{s^3-s}\tau^3\right)\approx-\frac{4}{s}H(2H-1)\left(\frac{1}{2H-1}s^{2H-1}-\frac{2}{2H}s^{2H-1}+\frac{1}{2H+2}s^{2H-1}\right)$$
$$=-4H(2H-1)\frac{2(2-H)}{2H(2H-1)(2H+2)}s^{2H-2}=-2\frac{2-H}{H+1}s^{2H-2}. \tag{A23}$$

After plugging (A17) and (A23) into (A16) finally we obtain Eq. (23).

5. Example: Ordinary Brownian motion

Using Eq. (16) for OBM, we obtain the following:

$$E[F^2(s)]=\frac{2}{s[N/s]}\sum_{v=1}^{[N/s]}\sum_{k=1}^{s}(k+d_v)\sum_{j=1}^{s}[\delta_{k,j}-P_1(k,j)]^2+\frac{2}{s[N/s]}\sum_{v=1}^{[N/s]}\sum_{k=1}^{s-1}\sum_{i=k+1}^{s}(k+d_v)\sum_{j=1}^{s}[\delta_{k,j}-P_1(k,j)][\delta_{i,j}-P_1(i,j)]. \tag{A24}$$

First we will show that

$$\sum_{j=1}^{s}[\delta_{i,j}-P_1(i,j)][\delta_{k,j}-P_1(k,j)]=\delta_{i,k}-2P_1(i,k)+\sum_{j=1}^{s}P_1(i,j)P_1(k,j). \tag{A25}$$

Indeed, For $k\neq i$ the left-hand side of (A25) is given by

$$\sum_{j=1}^{s}[\delta_{i,j}-P_1(i,j)][\delta_{k,j}-P_1(k,j)]=-[1-P_1(i,i)]P_1(k,i)-[1-P_1(k,k)]P_1(i,k)+\sum_{j=1,j\neq i,j\neq k}^{s}P_1(i,j)P_1(k,j)$$
$$=-2P_1(i,k)+\sum_{j=1}^{s}P_1(i,j)P_1(j,k).$$

For $k=i$ the left-hand side of (A25) takes the form

$$\sum_{j=1}^{s}[\delta_{i,j}-P_1(i,j)][\delta_{i,j}-P_1(i,j)]=[1-P_1(i,i)]^2+\sum_{j=1,j\neq i}^{s}P_1(i,j)P_1(i,j)=1-2P_1(i,i)+\sum_{j=1}^{s}P_1(i,j)P_1(i,j).$$

Thus, using Eqs. (A12) and (A25), the formula (A24) takes the form

$$E[F^2(s)]=\frac{1}{s[N/s]}\sum_{v=1}^{[N/s]}\sum_{k=1}(k+d_v)\left(1-2P_1(k,k)+\sum_{j=1}^{s}P_1(k,j)^2\right)$$
$$+\frac{2}{s[N/s]}\sum_{v=1}^{[N/s]}\sum_{k=1}^{s-1}\sum_{i=k+1}^{s}(k+d_v)\left(-2P_1(k,i)+\sum_{j=1}^{s}P_1(k,j)P_1(i,j)\right). \tag{A26}$$

Applying the definition of the $P_1(\cdot,\cdot)$ function given in (8) for $q=0$ and in (9) for $q=1$ to Eq. (A26) and using MATHEMATICA, we obtain formulas (25) and (26).

6. Example: Fractional Brownian motion

Using Eqs. (11), (16), and (27) we obtain

$$E[F^2(s)]=\frac{1}{s[N/s]}\sum_{v=1}^{[N/s]}\sum_{j=1}^{s}E\big[Y_v^2(j)\big]=\frac{1}{s[N/s]}\sum_{v=1}^{[N/s]}\sum_{j,i,k=1}^{s}E[X_3(i+d_v)X_3(k+d_v)][\delta_{i,j}-P_1(i,j)][\delta_{k,j}-P_1(k,j)]$$
$$=\frac{2}{s[N/s]}\sum_{v=1}^{[N/s]}\sum_{i,k=1}^{s}[i+(v-1)s]^{2H}\sum_{j=1}^{s}[\delta_{i,j}-P_1(i,j)][\delta_{k,j}-P_1(k,j)]$$
$$-\frac{1}{s}\sum_{k,i=1}^{s}|i-k|^{2H}\sum_{j=1}^{s}[\delta_{i,j}-P_1(i,j)][\delta_{k,j}-P_1(k,j)]=A(s)+B(s), \tag{A27}$$

where $P_1(\cdot,\cdot)$ is given in (8) for $q=0$ and in (9) for $q=1$, and

$$A(s) := \frac{2}{s[N/s]}\sum_{v=1}^{[N/s]}\sum_{i,k=1}^{s}[i+(v-1)s]^{2H}\sum_{j=1}^{s}[\delta_{i,j}-P_1(i,j)][\delta_{k,j}-P_1(k,j)], \tag{A28}$$

$$B(s) := -\frac{1}{s}\sum_{k,i=1}^{s}|i-k|^{2H}\sum_{j=1}^{s}[\delta_{i,j}-P_1(i,j)][\delta_{k,j}-P_1(k,j)]. \tag{A29}$$

In the case $q=0$ for large s, by using Eq. (A21) we have

$$\begin{aligned}B(s) &= -\frac{1}{s}\sum_{k,i=1}^{s}|i-k|^{2H}\left(\delta_{i,k}-\frac{1}{s}\right)\\ &= \frac{2}{s^2}\sum_{\tau=1}^{s-1}\sum_{i=1}^{s-\tau}|\tau|^{2H} = \frac{2}{s^2}\sum_{\tau=1}^{s-1}|\tau|^{2H}(s-\tau)\\ &\approx \frac{2(s-1)^{2H+1}}{s(2H+1)}-\frac{2(s-1)^{2H+2}}{s^2(2H+2)}\\ &\approx s^{2H}\left(\frac{2}{2H+1}-\frac{2}{2H+2}\right)\\ &= \frac{2s^{2H}}{(2H+1)(2H+2)},\end{aligned} \tag{A30}$$

$$\begin{aligned}A(s) &\approx \frac{2}{N}\sum_{v=1}^{N/s}\sum_{i,k=1}^{s}[i+(v-1)s]^{2H}\left(\delta_{i,k}-\frac{1}{s}\right)\\ &= \frac{2}{N}\sum_{v=1}^{N/s}\sum_{i=1}^{s}[i+(v-1)s]^{2H}\sum_{k=1}^{s}\left(\delta_{i,k}-\frac{1}{s}\right).\end{aligned} \tag{A31}$$

Observe that

$$\sum_{k=1}^{s}\left(\delta_{i,k}-\frac{1}{s}\right)=0;$$

thus we may neglect the contribution of $A(s)$ at large s. Finally we obtain (28).

We will show that in the case $q=1$ for large s the following holds:

$$A(s)\approx C_1 \quad \text{and} \quad B(s)\approx s^{2H}, \tag{A32}$$

where C_1 is some positive constants. Using formula (9) one can show that

$$\begin{aligned}P_1(i,t) &= \frac{2(2s+1)}{s(s-1)}+\frac{12it}{s(s-1)(s+1)}-\frac{6(t+i)}{s(s-1)}\\ &= \frac{4}{s-1}+\frac{2}{s(s-1)}\\ &\quad+\frac{6i(t-s-1)}{s(s-1)(s+1)}+\frac{6t(i-s-1)}{s(s-1)(s+1)}.\end{aligned} \tag{A33}$$

Observe that for $1\leqslant i,t\leqslant s$ and large s we have the following:

$$\begin{aligned}\left|\frac{6i(t-s-1)}{s(s-1)(s+1)}\right| &= \frac{6i(s+1-t)}{s(s-1)(s+1)}\\ &\leqslant \frac{6s^2}{s(s-1)(s+1)}\approx\frac{6}{s}.\end{aligned} \tag{A34}$$

We have a similar result for $|\frac{6t(i-s-1)}{s(s-1)(s+1)}|$. Thus one can conclude that $P_1(t,s)$ tends to zero as $\frac{1}{s}$ when s is large. We assume $P_1(i,t)\approx\frac{E_1}{s}$, where E_1 is some constant. Therefore, using Eq. (A25) we obtain for large s

$$\begin{aligned}B(s) &\approx -\frac{1}{s}\sum_{k,i=1}^{s}|i-k|^{2H}\left(\delta_{i,k}-\frac{2E_1}{s}+\sum_{j=1}^{s}\frac{E_1^2}{s^2}\right)\\ &= -\frac{1}{s}\sum_{k,i=1}^{s}|i-k|^{2H}\left(\delta_{i,k}-\frac{2E_1-E_1^2}{s}\right)\\ &= \frac{2\left(E_1-E_1^2\right)}{s^2}\sum_{\tau=1}^{s-1}\sum_{i=1}^{s-\tau}|\tau|^{2H}\\ &= \frac{2\left(2E_1-E_1^2\right)}{s^2}\sum_{\tau=1}^{s-1}(s-\tau)|\tau|^{2H}\\ &= \frac{2\left(2E_1-E_1^2\right)}{s}\sum_{\tau=1}^{s-1}|\tau|^{2H}-\frac{2\left(2E_1-E_1^2\right)}{s^2}\sum_{\tau=1}^{s-1}|\tau|^{2H+1}.\end{aligned} \tag{A35}$$

Using (A21) we obtain that, for large s, $B(s)$ tends to infinity as s^{2H}. In order to prove the behavior of $A(s)$ for large s we use reasonings similar to those for $B(s)$ behavior, namely

$$\begin{aligned}A(s) &\approx \frac{2}{N}\sum_{v=1}^{N/s}\sum_{i,k=1}^{s}[i+(v-1)s]^{2H}\left(\delta_{i,k}+\frac{E_1^2-2E_1}{s}\right)\\ &= \frac{2}{N}\sum_{v=1}^{N/s}\sum_{i=1}^{s}[i+(v-1)s]^{2H}\sum_{k=1}^{s}\left(\delta_{i,k}+\frac{E_1^2-2E_1}{s}\right)\\ &= \frac{2}{N}\sum_{v=1}^{N/s}\sum_{i=1}^{s}[i+(v-1)s]^{2H}\\ &\quad+\frac{2(E_1^2-2E_1)}{N}\sum_{v=1}^{N/s}\sum_{i=1}^{s}[i+(v-1)s]^{2H}\\ &= \frac{2(E_1-1)^2}{N}\sum_{v=1}^{N/s}\sum_{i=1+(v-1)s}^{vs}|i|^{2H}\\ &= \frac{2(E_1-1)^2}{N}\sum_{v=1}^{N/s}\sum_{i=1}^{vs}|i|^{2H}\\ &\quad-\frac{2(E_1-1)^2}{s}\sum_{v=1}^{N/s}\sum_{i=1}^{(v-1)s}|i|^{2H}.\end{aligned} \tag{A36}$$

Now, using (A21) we obtain

$$A(s) \approx \frac{2(E_1^2-1)^2}{N}\sum_{v=1}^{N/s}\frac{(vs)^{2H+1}}{2H+1} - \frac{2(E_1-1)^2}{N}\sum_{v=1}^{N/s}\frac{[(v-1)s]^{2H+1}}{2H+1}$$
$$= \frac{2(E_1-1)^2 s^{2H+1}}{N(2H+1)(2H+2)}\left(\left(\frac{N}{s}\right)^{2H+2} - \left(\frac{N}{s}-1\right)^{2H+2}\right)$$
$$= \frac{2(E_1-1)^2 s^{2H+1}}{N(2H+1)(2H+2)}\left(\frac{N}{s}\right)^{2H+2}\left(1-\left(1-\frac{s}{N}\right)^{2H+2}\right). \quad \text{(A37)}$$

Thus, taking the fact that for $s \ll N$

$$1-\left(1-\frac{s}{N}\right)^{2H+2} \approx (2H+2)\frac{s}{N}, \quad \text{(A38)}$$

we get

$$A(s) \approx \frac{2(E_1-1)^2 s^{2H+1}}{N(2H+1)(2H+2)}\left(\frac{N}{s}\right)^{2H+2}(2H+2)\frac{s}{N}$$
$$= \frac{2(E_1-1)^2 N^{2H}}{(2H+1)} = C_1, \quad \text{(A39)}$$

where C_1 is some positive constant. After taking the comment below Eq. (A35) and the formula (A39), finally we obtain Eq. (29).

[1] C. K. Peng, S. V. Buldyrev, S. Havlin, M. Simons, H. E. Stanley, and A. L. Goldberger, Phys. Rev. E **49**, 1685 (1994).
[2] K. Hu, P. C. Ivanov, Z. Chen, P. Carpena, and H. E. Stanley, Phys Rev. E **64**, 011114 (2001).
[3] J. W. Kantelhardt, E. Koscielny-Bunde, H. H. A. Rego, S. Havlin, and A. Bunde, Physica A **295**, 441 (2001).
[4] Z. Chen, P. C. Ivanov, K. Hu, and H. E. Stanley, Phys. Rev. E **65**, 041107 (2002).
[5] L. M. Xu, P. C. Ivanov, K. Hu, Z. Chen, A. Carbone, and H. E. Stanley, Phys. Rev. E **71**, 051101 (2005).
[6] Z. Chen, K. Hu, P. Carpena, P. Bernaola-Galvan, H. E. Stanley, and P. C. Ivanov, Phys. Rev. E **71**, 011104 (2005).
[7] A. Bashan, R. Bartsch, J. W. Kantelhardt, and S. Havlin, Physica A **387**, 5080 (2008).
[8] Q. D. Y. Ma, R. P. Bartsch, P. Bernaola-Galvan, M. Yoneyama, and M. P. C. Ivanov, Phys. Rev. E **81**, 031101 (2010).
[9] J. Beran, *Statistics of Long Memory Processes* (Chapman & Hall/CRC, Boca Raton, FL, 1994).
[10] J. Beran, Adv. Rev. **2**, 26 (2010).
[11] M. Höll and H. Kantz, Eur. Phys. J. B **88**, 327 (2015).
[12] M. Höll and H. Kantz, Eur. Phys. J. B **88**, 126 (2015).
[13] J. M. Bardet and I. Kammoun, IEEE Trans. Inf. Theory **54**, 2041 (2008).
[14] M. S. Taqqu, V. Teverovsky, and W. Wilinger, Fractals **03**, 785 (1995).
[15] M. S. Movahed, G. R. Jafari, F. Ghasemi, S. Rahvar, and M. R. R. Tabar, J. Stat. Mech. (2006) P02003.
[16] M. S. Movahed and E. Hermanis, Physica A **387**, 915 (2008).
[17] M. Höll, H. Kantz, and Y. Zhou, Phys. Rev. E **94**, 042201 (2016).
[18] C. Heneghan and G. McDarby, Phys. Rev. E **62**, 6103 (2000).
[19] K. Kiyono, Phys. Rev. E **92**, 042925 (2015).
[20] K. Kiyono and Y. Tsujimoto, Phys. Rev. E **94**, 012111 (2016).
[21] K. Kiyono and Y. Tsujimoto, Physica A **462**, 807 (2016).
[22] P. Talkner and R. O. Weber, Phys. Rev. E **62**, 150 (2000).
[23] K. Willson, D. P. Francis, R. Wensel, A. J. Coats, and K. H. Parker, Physiol. Meas. **23**, 385 (2002).
[24] K. Willson and D. P. Francis, Physiol. Meas. **24**, N1 (2003).
[25] O. Løvsletten, Phys. Rev. E **96**, 012141 (2017).
[26] M. Höll, K. Kiyono, and H. Kantz, Phys. Rev. E **99**, 033305 (2019).
[27] N. Crato, R. R. Linhares, and R. C. Lopes, J. Stat. Comput. Simul. **80**, 625 (2010).
[28] J. Gajda, A. Wylomanska, H. Kantz, A. V. Chechkin, and G. Sikora, Stat. Probab. Lett. **143**, 47 (2018).
[29] A. M. Mathai and S. B. Provost, *Quadratic Forms in Random Variables: Theory and Applications* (Marcel Dekker, New York, 1992).
[30] R. A. Horn and C. R. Johnson, *Matrix Analysis*, 2nd ed. (Cambridge University Press, Cambridge, 2013).
[31] P. G. Moschopoulos, Ann. Inst. Stat. Math. **37**, 541 (1985).
[32] V. Pipiras and M. S. Taqqu, *Long-Range Dependence and Self-Similarity* (Cambridge University Press, Cambridge, 2017).
[33] O. Y. Sliusarenko, V. Y. Gonchar, A. V. Chechkin, I. M. Sokolov, and R. Metzler, Phys. Rev. E **81**, 041119 (2010).
[34] A. Wyłomańska, A. Chechkin, J. Gajda, and I. M. Sokolov, Physica A **421**, 412 (2015).
[35] E. Alessio, A. Carbone, G. Castelli, and V. Frappietro, Eur. Phys. J. B **27**, 197 (2002).
[36] S. Arianos, A. Carbone, and C. Türk, Phys. Rev. E **84**, 046113 (2011).
[37] A. Carbone, in *IEEE TIC-STH 09: IEEE Toronto International Conference on Science and Technology for Humanity, Toronto*, 2009 (IEEE, Piscataway, NJ, 2009), p. 691.
[38] G. Sikora, Chaos Solitons Fractals **116**, 54 (2018).
[39] J. W. Kantelhardt, S. A. Zschiegner, E. Koscielny-Bunde, S. Havlin, A. Bunde, and H. E. Stanley, Physica A **316**, 87 (2002).
[40] G.-F. Gu and W.-X. Zhou, Phys. Rev. E **82**, 011136 (2010).
[41] A. Carbone, G. Castelli, and H. E. Stanley, Phys. A **344**, 267 (2004).
[42] T. Di Matteo, Quant. Finance **7**, 21 (2007).
[43] A. Serletis and A. A. Rosenberg, Physica A **380**, 325 (2007).
[44] R. Matsushita, I. Gleria, A. Figueiredo, and S. Da Silva, Phys. Lett. A **368**, 173 (2007).
[45] A. Serletis and A. A. Rosenberg, Chaos Solitons Fractals **40**, 2007 (2009).

[46] A. Carbone, Phys. Rev. E **76**, 056703 (2007).
[47] A. Carbone, B. M. Chiaia, B. Frigo, and C. Türk, Phys. Rev. E **82**, 036103 (2010).
[48] C. Türk, A. Carbone, and B. M. Chiaia, Phys. Rev. E **81**, 026706 (2010).
[49] A. K. Tiwari, G. C. Aye, and R. Gupta, Finance Res. Lett. **28**, 398 (2019).
[50] A. Burgueno, X. Lana, C. Serra, and M. D. Martinez, Phys. Lett. A **378**, 874 (2014).
[51] P. Mali, J. Stat. Mech. Theory Exp. (2016) 013201.
[52] D. B. de Freitas, M. M. F. Nepomuceno, J. G. Cordeiro, M. L. Das Chagas, and J. R. De Medeiros, Mon. Not. R. Astron. Soc. **488**, 3274 (2019).
[53] L. Isserlis, Biometrika **12**, 134 (1918).